J Anim Reprod Biotechnol 2023;38:291-299
pISSN: 2671-4639 • eISSN: 2671-4663
https://doi.org/10.12750/JARB.38.4.291

Original Article

Expression of TASK-1 channel in mouse Leydig cells

Min Seok Woo[1], Eun-Jin Kim[1], Anjas Happy Prayoga[1,2], Yangmi Kim[3] and Dawon Kang[1,2,*]

[1]Department of Physiology, College of Medicine and Institute of Medical Sciences, Gyeongsang National University, Jinju 52727, Korea
[2]Department of Convergence Medical Science, Gyeongsang National University, Jinju 52727, Korea
[3]Department of Physiology, Chungbuk National University College of Medicine, Cheongju 28644, Korea

Received November 30, 2023
Revised December 12, 2023
Accepted December 12, 2023

***Correspondence**
Dawon Kang
E-mail: dawon@gnu.ac.kr

Author's Position and Orcid no.
Woo MS, Post-doctoral fellow,
https://orcid.org/0000-0002-0357-9666
Kim E-J, Postdoctoral fellow,
https://orcid.org/0000-0003-1068-9334
Prayoga AH, MS student,
https://orcid.org/0009-0007-0910-4788
Kim Y, Professor,
https://orcid.org/0000-0003-1536-116X
Kang D, Professor,
https://orcid.org/0000-0001-7402-7298

ABSTRACT

Background: Leydig cells, crucial for testosterone production, express ion channels like ANO1 that influence hormone secretion. This study investigates the expression and role of the Tandem of P domains in a weak inward rectifying K^+ channel-related Acid-Sensitive K^+-1 (TASK-1) channel in these cells, exploring its impact on testicular function and steroidogenesis.

Methods: TASK-1 expression in Leydig cells was confirmed using immunostaining, while RT-PCR and Western Blot (WB) validated its expression in the TM3 Leydig cell line. The effect of a TASK-1 channel blocker on cell viability was assessed through live/dead staining and MTT assays. Additionally, the blocker's effect on testosterone secretion was evaluated by measuring testosterone levels.

Results: Immunohistochemical analysis revealed a predominant presence of TASK-1, along with c-Kit and ANO-1, in Leydig cells adjacent to seminiferous tubules and also in Sertoli and spermatogenic cells. Expression levels of TASK-1 mRNA and protein were significantly higher in TM3 Leydig cells compared to TM4 Sertoli cells. In addition, blocking TASK-1 in TM3 cells with ML365 induced cell death but did not affect LH-induced testosterone secretion.

Conclusions: These findings suggest that TASK-1 in Leydig cells is crucial for their viability and proliferation, highlighting its potential importance in testicular physiology.

Keywords: cell death, Leydig cells, mice, TASK-1, testosterone

INTRODUCTION

Leydig cells are located in the interstitial tissue of the testes and are responsible for producing and secreting testosterone. Testosterone is essential for the development of male reproductive structure, secondary sexual characteristics, and overall physiology. Gene expression patterns in Leydig cells affect testosterone levels, which in turn affect germ cell proliferation and maturation, and thus spermatogenesis (O'Shaughnessy et al., 2002; Jauregui et al., 2018). Our recent study found that Leydig cells express c-Kit, a receptor tyrosine kinase Kit, and anoctamin 1 (ANO1), a Ca^{2+}- dependent Cl^- channel. The c-Kit and ANO1 affect testosterone secretion (Ko et al., 2022).

Leydig cells express ion channels and show membrane potential activity affecting hormone production, although Leydig cells differ from excitable cells like neurons and muscles (Poletto Chaves and Varanda, 2008; Zhou et al.,

2011; Matzkin et al., 2013). The electrical properties of Leydig cells are primarily related to their responsiveness to hormonal signals and their involvement in the synthesis and secretion of testosterone. While they lack typical excitability, control of membrane potential and ion channel activity is crucial for testosterone secretion. In our previous study, LH induced an increase in intracellular Ca^{2+} concentration, membrane depolarization, and testosterone secretion (Ko et al., 2022). The link between membrane depolarization and testosterone secretion suggest that depolarization by ion channel modulation may cause testosterone to be secreted.

Tandem of P domains in a Weakly Inward rectifying K^+ channel (TWIK)-related Acid-Sensitive K^+ (TASK)-1 channel is the most prominently expressed of the 93 K^+ channel subunits in mouse jejunal interstitial cells of Cajal (ICC) (Lee et al., 2017). Leydig cells are another type of interstitial cells. TASK-1 channels exert significant influence over the establishment and maintenance of cells' resting membrane potential. In particular, these channels are sensitive to changes in oxygen concentration and pH (Kim et al., 2009). Furthermore, their activity is inhibited by a range of hormones including serotonin, norepinephrine, substance P, and thyrotropin-releasing hormone (Talley et al., 2000). A recent study demonstrated that TASK-1 mRNA was detected in Leydig cells (Guan et al., 2022). However, its specific role within the testes and in steroidogenesis remains unidentified. Our study aimed to identify the expression of TASK-1 channel and its potential regulatory function in mouse Leydig cells.

MATERIALS AND METHODS

Chemicals

Chemicals and culture media were primarily sourced from Sigma Chemical Co., located in St. Louis, MO, USA, unless stated otherwise. Luteinizing hormone (LH, 25 units/mL) and ML365 (100 mM) were dissolved in distilled water and dimethyl sulfoxide (DMSO), respectively, to create the stock solution. In the culture medium, these compounds were diluted to their required working concentrations. Whenever DMSO was utilized as a solvent, a control solution of equivalent concentration was employed. It was ensured that the final concentration of DMSO in the working solutions did not exceed 0.1%.

Animals and testis isolation

Male mice of the C57BL/6 strain, aged six weeks, were procured from Central Lab. Animal Inc. (Seoul, Korea). These mice were maintained in a pathogen-free environment with ad libitum access to food and water and subjected to a 12-h light-dark cycle for one week. At the age of seven weeks, testes were isolated from these mice. The handling and experimental procedures involving these animals were conducted in compliance with the guidelines set by the Gyeongsang National University Animal Care and Use Committee (GNU-200702-M0041).

Hematoxylin and eosin (H&E) staining

For the histological examination of testes, hematoxylin and eosin (H&E) staining was performed, following the protocol described in the previous study (Siregar et al., 2019). Testicular tissues were fixed in a 4% paraformaldehyde solution overnight at 4℃, followed by washing in 0.1 M PBS. These tissues were then embedded in paraffin and sectioned into 5 μm-thick slices. The paraffin sections, once air-dried on gelatin-coated slides, were deparaffinized and rinsed with tap water. Staining with hematoxylin solution was carried out for 5 min, followed by eosin staining for the same duration. A series of alcohol dehydrations (from 70% to 100% ethanol, each for 3 min) and xylene clearance were performed. Permount mounting media (Fisher Chemical, Geel, Belgium) was used for mounting the sections. An Olympus BX61VS microscope (Tokyo, Japan) was employed to examine and photograph the stained sections. Five different sections from each sample were analyzed to ensure consistency.

Immunohistochemistry (IHC)

Tissue sections, after deparaffinization, were treated with 0.2% Triton X-100 for 10 min at room temperature to allow permeabilization. Post three washes with PBS, the sections underwent a 60-min incubation at room temperature in a blocking solution composed of 10% normal goat serum in 0.1 M PBS. Subsequently, they were incubated with primary antibodies against TASK-1 (polyclonal anti-rabbit KCNK3, Alomone Labs™, Jerusalem, Israel), c-Kit (Alexa Fluor® 594 anti-mouse CD117, Biolegend, San Diego, CA, USA), and ANO1 (monoclonal anti-mouse TMEM16A antibody, Santa Cruz Biotechnology, Dallas, TX, USA) at a 1:100 dilution, overnight at 4℃. Following this, the sections were exposed to fluorescein isothiocya-

nate (FITC)-conjugated anti-rabbit IgG secondary antibody (Abcam, Cambridge, UK) and anti-mouse IgG Texas red® (Abcam), diluted 1:400 in PBS, for 1.5 hours in the dark, with three intervening PBS washes. After PBS washes, nuclear staining was performed using 4',6'-diamidino-2-phenylindole (DAPI). Gel/Mount™ (Biomeda Corp., Foster City, CA, USA) was used for wet-mounting the stained sections, which were then examined under a confocal laser scanning microscope (Olympus, Tokyo, Japan).

Cell culture

The TM3 mouse Leydig cell line (American Type Culture Collection, Manassas, VA, USA) was generously provided by Dr. Jung Hye Shin (Namhae Garlic Research Institute, Namhae, Korea). The TM4 mouse Sertoli cell line was acquired from the Korean Cell Line Bank (Seoul, Korea). Cell culture methods were in accordance with those described in the previous study (Yang et al., 2019). Cultivation of the cells was in Dulbecco's Modified Eagle's Medium (DMEM; Gibco/Life technologies, Grand Island, NY, USA), enriched with 10% fetal bovine serum (FBS; Gibco), 100 U/mL penicillin (Gibco), and 100 mg/mL streptomycin (Gibco). These cells were maintained at 37℃ in a gas combination of 95% air and 5% CO_2, with media replacements occurring every two days.

Total RNA extraction

Total RNA was extracted from TM3 and TM4 cells using TRIzol™ Reagent (Invitrigen, Carlsbad, CA, USA), following the manufacturer's protocol and procedures as previously described (Siregar et al., 2019).

Briefly, cells washed with 1× PBS were lysed directly in the culture dish using TRIzol™ (Invitrogen). The lysate was incubated at room temperature for 5 min, mixed with chloroform, and centrifuged. The RNA was then precipitated from the aqueous phase with isopropanol, washed with 75% ethanol, and resuspended in diethyl pyrocarbonate (DEPC)-treated RNase-free water.

Reverse transcriptase-polymerase chain reaction (RT-PCR)

cDNA synthesis was performed using the DiaStart™ RT kit (SolGent, Daejeon, Korea) with 3 μg of total RNA. PCR amplification employed specific primers for mouse *KCNK3* (NM_010608.3, forward: 5'- TCCTTCTACTTCGCCATCACC -3' and reverse: 5'- AGCAGGTACCTCACGAAGGTGT -3': 173 bp) and glyceraldehydes-3-phosphate dehydrogenase (*GAPDH,* BC096042.1, forward: 5' - TGTCATCAACGGGAAGC -3' and reverse: 5'-GGAGATGATGACCCGTTT-3'; 166 bp). The protocol included an initial denaturation (94℃, 5 min), followed by 35 cycles of amplification (94℃, 30 sec -59℃, 30 sec -72℃, 30 sec), and a final extension (72℃, 10 min). PCR products were analyzed on a 1.5% agarose gel using the iBright™ CL1500 system (Thermo Scientific Fisher/Life Technologies Holdings Pte Ltd., Singapore) and sequenced with the ABI PRISM® 3100-Avant Genetic Analyzer (Applied Biosystems, CA, USA).

Western blot analysis

Western blotting was performed according to the method described earlier (Yang et al., 2019). TM3 cells, at a density of 5×10^4 cells per 60-mm dish. To extract proteins, cells were lysed with RIPA buffer (Thermo Fisher Scientific., Waltham, MA, USA) supplemented with a protease inhibitor cocktail (Roche Diagnostics., Indianapolis, IN, USA), followed by centrifugation at 15,871 ×g for 20 min at 4℃. Protein concentrations in the lysates were quantified using the Pierce bicinchoninic acid (BCA) protein assay kit (Thermo Fisher Scientific). Proteins were then separated on an 8% sodium dodecyl sulfate (SDS)-polyacrylamide gel and transferred to a polyvinylidene difluoride (PVDF) membrane (Millipore, Billerica, MA, USA). After blocking with 5% fat-free milk in tris buffered saline with Tween20 (TBST), membranes were incubated overnight at 4℃ with anti-TASK-1 (Alomone Labs™) and anti-β-actin antibodies. Following incubation with horseradish peroxidase (HRP)-conjugated secondary antibodies (Assay Designs, Ann Arbor, MI, USA), detection was performed using enhanced chemiluminescence (Thermo Fisher Scientific) and imaged with the iBright™ CL1500 system. β-actin served as the loading control for protein level normalization.

Live/dead cell staining

Live/dead cell staining was performed as previously described (Yang et al., 2019). Live cells stained with Calcein-AM (Thermo Fisher Scientific, Eugene, OR, USA) appear green, while dead cells stained with propidium iodide (PI) appear red. TM3 cells (5×10^3 cells/100 μL) were cultured in glass-bottom culture dish (SPL, Pocheon, Korea) for 24 h, followed by a 24-h treatment with 1 μM ML365. After

two washes with Opti-MEM, cells were stained with 3 μM calcein-AM and 3 μg/mL PI for 25 min at room temperature. Post-wash, stained cells were examined using a confocal laser scanning microscope (Olympus, Tokyo, Japan), with filters for Texas Red and FITC.

Cell viability assay

The viability of TM3 cells treated with ML365 was assessed using a 3-(4,5-dimethylthiazole-2-yl)-2,5-diphenyl tetrazolium bromide (MTT) assay, employing a reagent (Duchefa Biochemie, Haarlem, Netherlands) concentration of 5 mg/mL in PBS. This assay was performed as previously described (Yang et al., 2019). TM3 cells were plated at a density of 5×10^3 cells/well in 100 μL culture medium in 96-well plates and allowed to grow for 24 h prior to chemical treatment. The treatments were applied for 24 h. Subsequently, 10 μL of MTT solution (5 mg/mL, Duchefa Biochemie) was added to each well and the plates were incubated for 2 h at 37℃ in a dark environment. Afterward, the supernatants were carefully removed, and the formazan crystals formed in each well were dissolved in 100 μL DMSO. This was facilitated by shaking the plates for 10 min at room temperature. The absorbance of each well was then measured at 570 nm using a VERSAmax™ microplate reader (Molecular Devices, San Jose, CA, USA).

Measurement of testosterone concentration

Testosterone levels in the supernatants of TM3 cell cultures were measured using a testosterone parameter assay kit (R&D Systems, Minneapolis, MN, USA), following the guidelines provided by the manufacturer. Briefly, TM3 cells were cultured in DMEM (Gibco) at a density of 5×10^4 cells/mL in 24-well plates for 24 h. The cells were then subjected to serum-free DMEM (Gibco) and exposed to LH either alone or combined with ML365. Post-treatment, the cell culture medium was collected, and the supernatant was separated using centrifugation at 11,340 × *g* for 10 min using an Eppendorf centrifuge (Hamburg, Germany). The assay procedure included the addition of 50 μL of the primary antibody solution to each well and an incubation period of 1 h with shaking at room temperature. This was followed by three washes, after which 100 μL of calibrator diluent was added to the wells designated for non-specific binding and zero standards. The remaining wells received either the standard, control, or sample. Each well then received 50 μL of conjugate solution and was incubated for 3 h with shaking. Subsequently, the wells were treated with 200 μL of substrate solution for 30 min in a dark, room temperature environment. The reaction was halted by adding 50 μL of stop solution, and the optical density at 405 nm was immediately measured using a VERSAmax™ microplate reader (Molecular Devices). The testosterone concentrations were calculated based on the standard curve.

Statistical analysis

Data are presented as mean ± S.D. The differences between groups were assessed using the Student's *t*-test, utilizing OriginPro2020 software (OriginLab Corp., Northampton, MA, USA). A *p*-value of less than 0.05 was considered to indicate statistical significance.

RESULTS

TASK-1 is expressed in Leydig cells and Sertoli cells within the testes of mice

Hematoxylin and Eosin (H&E) staining was performed to examine testicular morphology. The seminiferous tubules displayed a normal structure, with clear visibility of spermatogenic cells, Sertoli cells, and Leydig cells. No pathological changes were detected in the seminiferous tubules (Fig. 1A, n = 3). We employed specific antibodies against TASK-1, c-Kit, and ANO-1 for immunohistochemical studies. The results indicated a predominant localization of c-Kit and ANO-1 in Leydig cells adjacent to the seminiferous tubules (Fig. 1B, n = 3). Particularly, cells positive for c-Kit and ANO-1 concurrently expressed TASK-1. Furthermore, TASK-1 expression was observed in both Sertoli cells and spermatogenic cells (Fig. 1B, yellow and red arrows). The expression levels of TASK-1, as quantified by fluorescent intensity (FI), were observed to be higher in Leydig cells compared to Sertoli cells (8.8 ± 2.3 vs 2.4 ± 1.1). In spermatogenic cells, TASK-1 exhibited high FI values (9.4 ± 2.2).

TASK-1 is more highly expressed in TM3 cells compared to TM4 cells

TASK-1 was found in spermatogenic cells, Sertoli cells, and Leydig cells in mouse testes (Fig. 1B). Given the previously established presence of TASK-1 in mouse sperm (Hur et al., 2009), our study focused on TASK-1 expression in

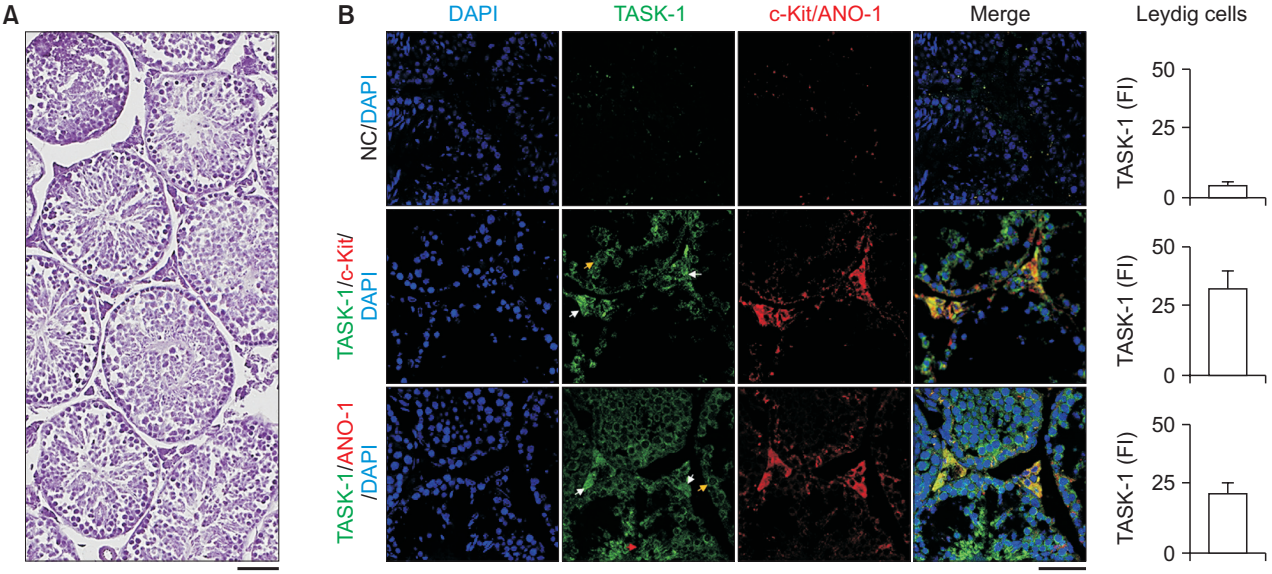

Fig. 1. Expression of TASK-1 in Leydig cells of mouse. (A) Histological analysis of testis. Hematoxylin and eosin (H&E) stained section showing the morphology of the testicular tissue with clearly visible cellular nuclei and cytoplasmic structures. (B) Immunofluorescence analysis of testis. Negative control (NC) with DAPI staining, where the blue fluorescence indicates the location of cell nuclei within the tissue sample. Co-localization of TASK-1 protein (green fluorescence) and c-Kit (red fluorescence) or ANO-1 (red fluorescence) with DAPI staining (blue fluorescence). Bar graphs indicate the normalized expression levels of TASK-1 relative to NC fluorescent intensity (FI). Each bar represents the mean ± SD from three independent experiments. The FI value is presented in arbitrary units (a.u.). White arrows point to Leydig cells, yellow arrows to Sertoli cells, and a red arrow to spermatogenic cells. Scale bars are set at 50 μm.

Leydig and Sertoli cells. Comparative analysis of TASK-1 expression in Leydig cell line TM3 and Sertoli cell line TM4 showed that TASK-1 mRNA and protein levels were significantly higher in TM3 cells than in TM4 cells (Fig. 2A and 2B, n = 3, $p < 0.05$).

Blocking TASK-1 induces death in TM3 cells

To investigate role of TASK-1 in TM3 cells, our study employed ML365, a known TASK-1 blocker. TM3 cells treated with 1 μM ML365 for 24 h exhibited a substantial decrease in TASK-1 protein levels (Fig. 3A). In addition, ML365 treatment led to cell death (Fig. 3B and 3C, n = 3). As shown in Fig. 3B, there was a high number of PI stained cells in the cells treated with ML365. In addition, MTT assay showed a significant decrease in cell viability following ML365 treatment ($p < 0.05$, Fig. 3C). In the testosterone secretion assay, the control group showed a testosterone concentration of 10.8 ± 0.5 pg/mL. Treatment with luteinizing hormone (LH) resulted in an approximate 5-fold increase in testosterone concentration. However, ML365 treatment did not have a significant effect on the LH-induced increase in testosterone secretion (Fig. 3D, n = 3).

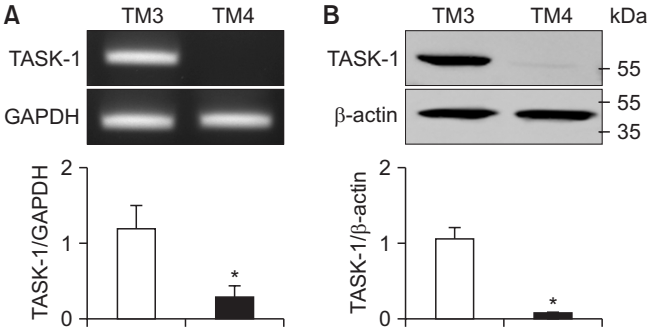

Fig. 2. Comparative TASK-1 expression levels in TM3 and TM4 cells. (A) PCR analysis of TASK-1 mRNA expression. The agarose gel electrophoresis image shows PCR bands for TASK-1 mRNA in TM3 and TM4 cell lines, with GAPDH serving as a loading control. The accompanying bar graph quantifies the relative expression of TASK-1, normalized to GAPDH levels. Each bar represents the mean ± SD from three independent experiments. (B) Protein expression analysis of TASK-1 via Western blot. The immunoblot bands demonstrate TASK-1 protein levels in TM3 and TM4 cells, with β-actin serving as a loading control. A bar graph indicates the normalized expression levels of TASK-1 relative to β-actin. Each bar represents the mean ± SD from three independent experiments. Statistical significance is denoted by *$p < 0.05$ when compared to TM3 cells.

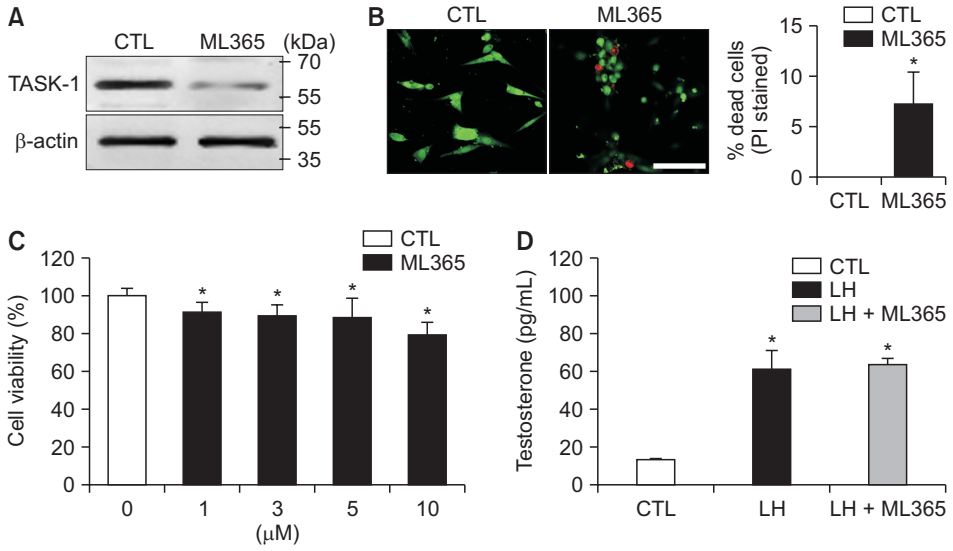

Fig. 3. Effect of TASK-1 blocker ML365 on cell viability and testosterone concentration in TM3 cells. (A) Decrease in TASK-1 protein levels by ML365 treatment. Western blot analysis illustrates the expression levels of TASK-1 and β-actin (as a loading control) in control (CTL) and ML365-treated TM3 cells. The molecular weights (kDa) are indicated on the right. (B) Effect of ML365 on cell viability. Live cells are indicated by green fluorescence (Calcein), and dead cells by red fluorescence (propidium iodide, PI). A bar graph displays the percentage of PI stained dead cells in relation to calcein-stained live cells. The scale bar represents 100 μm. (C) MTT assay. TM3 cells were incubated for 24 h with various concentrations of ML365. (D) Testosterone concentration. After 24 h of treatment with leutenizing hormone (LH) and/or ML365 in TM3 cells, the concentration of testosterone secreted was quantified. Each bar represents the mean ± SD from three independent experiments. *$p < 0.05$ compared to control.

DISCUSSION

Leydig cells express both c-Kit and ANO1 (Ko et al., 2022). The co-localization of TASK-1 with c-Kit and ANO-1 strongly argues that TASK-1 is expressed in Leydig cells. K^+ channels expressed in Leydig cells are involved in the maintenance of various cellular physiological functions through the regulation of resting membrane potential and ion concentrations, influencing testosterone release. TASK-1 channels are crucial in setting the resting membrane potential in excitable and non-excitable cells, and are modulated by various factors including pH, anesthetics, and other factors (Duprat et al., 1997; Bayliss et al., 2001). Given the predominant expression of TASK-1 in ICC, we hypothesized that it would also be present in Leydig interstitial cells. As expected, TASK-1 expression was indeed confirmed in Leydig cells. However, there are no reports specifying the exact physiological function of TASK-1 in the testis.

When comparing the mRNA and protein expression of TASK-1 in TM3 and TM4 cells, we observed a notably lower expression in TM4 cells. This finding contrasts with the established presence of TASK-1 in Sertoli cells within testicular tissue. Such discrepancies in TASK-1 expression between testicular tissue and cell lines might be attributed to the differing developmental stages of the cells being examined. TM3 and TM4, as immature cell types, exhibit a unique expression pattern when compared to the pattern observed in testicular tissues obtained from 6-week-old mice. Considering that these cell lines were established at approximately 2 weeks of age, it's plausible that the gene and protein expression profiles would significantly differ from those in more mature tissues. This suggests that TASK-1 expression undergoes developmental changes. In our study, we initially focused on the role of TASK-1 in Leydig cells, given its identification in both TM3 cells and Leydig cells in mouse testicular tissue. Further study is needed to investigate the changes in TASK-1 expression across various developmental stages and its specific roles in Sertoli cells.

TASK-1 is highly upregulated in the testis of neudesin-KO mouse. The absence of the neudesin gene led to a reduction in testicular size, however, it had no effect on the histological features or the spermatogenic function of the testis (Hasegawa et al., 2022). Hasegawa et al. (2022) did not verify the expression of TASK-1 in specific cell types, including Leydig cells and Sertoli cells. Increased TASK-1 expression in the testes may have affected the size of the

testes because it has the effect of reducing the volume. In this study, TASK-1 was preferentially expressed in Leydig cells over Sertoli cells, so the decrease in testicular size may be due to the role of neudesin and TASK-1 in Leydig cells.

TASK-1 channels are involved in the secretion of several classes of hormones and are regulated by hormones. TASK-1 is prominently expressed in the adrenal cortex (Nogueira et al., 2010; Bandulik et al., 2015) and is closely linked to aldosterone production (Nogueira et al., 2010; Bandulik et al., 2015). TASK-1 channels expressed in pancreatic α- and β-cells are involved in glucose metabolism and insulin secretion (Bramswig et al., 2013; Dadi et al., 2014; Dadi et al., 2015). In embryonic testes, exposure to estradiol has been shown to decrease the expression of TASK-1 (Cederroth et al., 2007). Moreover, the level of TASK-1 in decidual cells is affected by the estrogen and progesterone (Cloke et al., 2008). However, there are limited studies exploring the relationship between testosterone secretion and TASK-1 channels.

The discovery of TASK-1 expression in Leydig cells led us to examine its role in testosterone secretion, a fundamental function of these cells. However, contrary to our expectations, the LH-induced increase in testosterone secretion was not diminished by treatment with a TASK-1 blocker. This indicates that TASK-1 may not play a direct role in the secretion of testosterone. Nevertheless, we acknowledge the possibility that the TASK-1 blocker ML365, utilized in this study, might influence other channels that have not been identified here. Furthermore, further study should aim to explore the effects of modulating TASK-1 expression on testosterone secretion. Given the current study's limitations due to the absence of selective modulators, it is crucial to validate our findings through future studies employing a range of modulators.

The reported IC_{50} of ML365 for inhibiting TASK-1 channels is 4 nM (Zhou et al., 2011), indicating a high potency at very low concentrations. For our experiments, we opted for a 1 μM concentration of ML365. This choice was informed by results from the MTT assay, which indicated significant cell death at concentrations exceeding 1 μM. While the 1 μM concentration of ML365 did induce cell death, the rate was comparatively lower. Further study should focus on precisely evaluating the variations in testosterone secretion and the nature and degree of cell death at different concentrations of TASK-1 blockers like ML365, employing advanced molecular biological methods.

On the other hand, the application of TASK-1 blockers was found to induce death in Leydig cells. While the precise mechanism behind this induction of cell death was not examined in this study, it is plausible that blocking TASK-1 channels in Leydig cells could lead to cell death by causing an increase in intracellular calcium and mitochondrial dysfunction, which may result from the depolarization of the membrane potential. Cell death in TM3 cells, triggered by a range of harmful agents, is linked with mitochondrial fragmentation and dysfunction, as well as disturbances in Ca^{2+} homeostasis (Ham et al., 2020; Yi et al., 2022). Mitochondrial uncouplers stimulate cells by inhibiting K^+ conductance, including the background conductance of TASK-1, which results in membrane depolarization and the influx of Ca^{2+} through voltage-gated channels (Buckler and Vaughan-Jones, 1998).

The death of Leydig cells could potentially impact testosterone secretion, but it did not alter the level of testosterone production stimulated by LH. This could imply that while TASK-1 plays a role in cell survival, it might not be directly involved in the steroidogenic pathway of testosterone synthesis that LH stimulates. Alternatively, there could be compensatory mechanisms in Leydig cells that maintain testosterone production even when some cells undergo death. Further study should focus on elucidating the complex interplay between LH, testosterone, and TASK-1.

In conclusion, this study reports the distinct expression and significant role of TASK-1 in different cells of the mouse testis, particularly emphasizing its importance in Leydig cell viability and proliferation, and suggesting its potential effect on testicular function and health.

Author Contributions: Conceptualization, D.K.; data curation, M.S.W., E.J.K., A.H.P., and D.K.; formal analysis, M.S.W. and D.K.; funding acquisition, D.K.; investigation, M.S.W., E.J.K., A.H.P.; methodology, M.S.W. and D.K.; project administration, E.J.K.; supervision, Y.K., D.K.; validation, D.K.; visualization, M.S.W., D.K.; writing – original draft, Y.K., D.K.; writing – review & editing, D.K.

Funding: This work was supported by the Basic Science Research Program through the National Research

Foundation of Korea funded by the Ministry of Education (2021R1I1A3044128).

Ethical Approval: Not applicable.

Consent to Participate: Not applicable.

Consent to Publish: Not applicable.

Availability of Data and Materials: Not applicable.

Acknowledgements: None.

Conflicts of Interest: No potential conflict of interest relevant to this article was reported.

REFERENCES

Bandulik S, Tauber P, Lalli E, Barhanin J, Warth R. 2015. Two-pore domain potassium channels in the adrenal cortex. Pflugers Arch. 467:1027-1042.

Bayliss DA, Talley EM, Sirois JE, Lei Q. 2001. TASK-1 is a highly modulated pH-sensitive 'leak' K(+) channel expressed in brainstem respiratory neurons. Respir. Physiol. 129:159-174.

Bramswig NC, Everett LJ, Schug J, Dorrell C, Liu C, Luo Y, Streeter PR, Naji A, Grompe M, Kaestner KH. 2013. Epigenomic plasticity enables human pancreatic α to β cell reprogramming. J. Clin. Invest. 123:1275-1284.

Buckler KJ and Vaughan-Jones RD. 1998. Effects of mitochondrial uncouplers on intracellular calcium, pH and membrane potential in rat carotid body type I cells. J. Physiol. 513(Pt 3):819-833.

Cederroth CR, Schaad O, Descombes P, Chambon P, Vassalli JD, Nef S. 2007. Estrogen receptor alpha is a major contributor to estrogen-mediated fetal testis dysgenesis and cryptorchidism. Endocrinology 148:5507-5519.

Cloke B, Huhtinen K, Fusi L, Kajihara T, Yliheikkilä M, Ho KK, Teklenburg G, Lavery S, Jones MC, Trew G, Kim JJ, Lam EW, Cartwright JE, Poutanen M, Brosens JJ. 2008. The androgen and progesterone receptors regulate distinct gene networks and cellular functions in decidualizing endometrium. Endocrinology 149:4462-4474.

Dadi PK, Luo B, Vierra NC, Jacobson DA. 2015. TASK-1 potassium channels limit pancreatic α-cell calcium influx and glucagon secretion. Mol. Endocrinol. 29:777-787.

Dadi PK, Vierra NC, Jacobson DA. 2014. Pancreatic β-cell-specific ablation of TASK-1 channels augments glucose-stimulated calcium entry and insulin secretion, improving glucose tolerance. Endocrinology 155:3757-3768.

Duprat F, Lesage F, Fink M, Reyes R, Heurteaux C, Lazdunski M. 1997. TASK, a human background K+ channel to sense external pH variations near physiological pH. EMBO J. 16: 5464-5471.

Guan X, Chen P, Ji M, Wen X, Chen D, Zhao X, Huang F, Wang J, Shao J, Xie J, Zhao X, Chen F, Tian J, Lin H, Zirkin BR, Duan P, Su Z, Chen H. 2022. Identification of rat testicular Leydig precursor cells by single-cell-RNA-sequence analysis. Front. Cell Dev. Biol. 10:805249.

Ham J, Lim W, Whang KY, Song G. 2020. Butylated hydroxytoluene induces dysregulation of calcium homeostasis and endoplasmic reticulum stress resulting in mouse Leydig cell death. Environ. Pollut. 256:113421.

Hasegawa H, Kondo M, Nakayama K, Okuno T, Itoh N, Konishi M. 2022. Testicular hypoplasia with normal fertility in neudesin-knockout mice. Biol. Pharm. Bull. 45:1791-1797.

Hur CG, Choe C, Kim GT, Cho SK, Park JY, Hong SG, Han J, Kang D. 2009. Expression and localization of two-pore domain K(+) channels in bovine germ cells. Reproduction 137:237-244.

Jauregui EJ, Mitchell D, Garza SM, Topping T, Hogarth CA, Griswold MD. 2018. Leydig cell genes change their expression and association with polysomes in a stage-specific manner in the adult mouse testis. Biol. Reprod. 98:722-738.

Kim D, Cavanaugh EJ, Kim I, Carroll JL. 2009. Heteromeric TASK-1/TASK-3 is the major oxygen-sensitive background K+ channel in rat carotid body glomus cells. J. Physiol. 587(Pt 12):2963-2975.

Ko EA, Woo MS, Kang D. 2022. Testosterone secretion is affected by receptor tyrosine kinase c-Kit and anoctamin 1 activation in mouse Leydig cells. J. Anim. Reprod. Biotechnol. 37:87-95.

Lee MY, Ha SE, Park C, Park PJ, Fuchs R, Wei L, Jorgensen BG, Redelman D, Ward SM, Sanders KM, Ro S. 2017. Transcriptome of interstitial cells of Cajal reveals unique and selective gene signatures. PLoS One 12:e0176031.

Matzkin ME, Lauf S, Spinnler K, Rossi SP, Köhn FM, Kunz L, Calandra RS, Frungieri MB, Mayerhofer A. 2013. The Ca2+-activated, large conductance K+-channel (BKCa) is a player in the LH/hCG signaling cascade in testicular Leydig cells. Mol. Cell. Endocrinol. 367:41-49.

Nogueira EF, Gerry D, Mantero F, Mariniello B, Rainey WE. 2010. The role of TASK1 in aldosterone production and its expression in normal adrenal and aldosterone-producing adenomas. Clin. Endocrinol. (Oxf.) 73:22-29.

O'Shaughnessy PJ, Willerton L, Baker PJ. 2002. Changes in Leydig cell gene expression during development in the mouse. Biol. Reprod. 66:966-975.

Poletto Chaves LA and Varanda WA. 2008. Volume-activated chloride channels in mice Leydig cells. Pflugers Arch. 457: 493-504.

Siregar AS, Nyiramana MM, Kim EJ, Shin EJ, Kim CW, Lee DK, Hong SG, Han J, Kang D. 2019. TRPV1 is associated with testicular apoptosis in mice. J. Anim. Reprod. Biotechnol. 34: 311-317.

Talley EM, Lei Q, Sirois JE, Bayliss DA. 2000. TASK-1, a two-pore domain K+ channel, is modulated by multiple neurotransmitters in motoneurons. Neuron 25:399-410.

Yang JH, Siregar AS, Kim EJ, Nyiramana MM, Shin EJ, Han J, Sohn JT, Kim JW, Kang D. 2019. Involvement of TREK-1 channel in cell viability of H9c2 rat cardiomyoblasts affected by bupivacaine and lipid emulsion. Cells 8:454.

Yi L, Shang XJ, Lv L, Wang Y, Zhang J, Quan C, Shi Y, Liu Y, Zhang L. 2022. Cadmium-induced apoptosis of Leydig cells is mediated by excessive mitochondrial fission and inhibition of mitophagy. Cell Death Dis. 13:928.

Zhou M, He HJ, Tanaka O, Sekiguchi M, Kawahara K, Abe H. 2011. Different localization of ATP sensitive K+ channel subunits in rat testis. Anat. Rec. (Hoboken) 294:729-737.